Polaron Zeeman Effect in CdTe†

Daniel R. Cohn
Francis Bitter National Magnet Laboratory, Massachusetts Institute of Technology, Cambridge, Massachusetts 02139

and

David M. Larsen
Lincoln Laboratory, Massachusetts Institute of Technology, Lexington, Massachusetts 02173

and

Benjamin Lax*
Francis Bitter National Magnet Laboratory, Massachusetts Institute of Technology, Cambridge, Massachusetts 02139
(Received 15 November 1971)

Fourier-transform spectroscopy has been employed to observe the far-infrared absorption resulting from the $1s$ to $2p$ shallow-donor-impurity transitions in CdTe. At zero magnetic field the absorption was found to occur at 87.3 ± 0.3 cm^{-1}. This value compares very well with the prediction of the simple hydrogenic model for shallow-donor-impurity states. The Zeeman splitting of the $(1s \rightarrow 2p)$ transition was studied in magnetic fields as high as 165 kG. By using the magnetic field to tune energy of the $2p$, $m = +1$ state first into that of the $1s$ state plus one LO phonon and then into that of the $2p$, $m = -1$ state plus one LO phonon, it was possible to make the first quantitative determination of the effect of the electron–LO-phonon interaction upon bound electrons. The experimental results were found to be in good agreement with a theoretical calculation for the energy levels of bound polarons. Furthermore, the study of the magnetic field dependence of the $(1s \rightarrow 2p, m = \pm 1)$ transitions has also shown that there are no strong polaron effects due to the electron–TO-phonon interaction in CdTe.

I. INTRODUCTION

We have employed Fourier-transform spectroscopy to study the far-infrared optical properties of hydrogenic shallow-donor-impurity states in n-CdTe. There are two distinct areas of interest in this study. First of all, we wanted to investigate the CdTe donor-impurity transitions themselves since prior to our initial observation[1] these transitions had never been observed. Secondly, and more important, by studying the Zeeman splitting of the $(1s \rightarrow 2p)$ transition at high magnetic fields we were able to make the first quantitative determination of polaron shifts (i.e., shifts due to the electron–LO-phonon interaction) of the energy levels of a bound electron. We have also developed a novel theoretical approach which quantitatively accounts for observed polaron phenomenon.

This paper is organized in the following manner. In Sec. II we present the experimental observations of shallow-impurity transitions in n-CdTe and compare the experimental data with theoretical predictions based upon a hydrogenic model of the shallow-impurity states where no polaron effects have been included. Section III discusses qualitatively the experimental manifestations of the polaron interaction. Section IV describes a new theoretical calculation of polaron effects upon hydrogenic Zeeman structure. Finally in Sec. V a quantitative comparison between theory and experiment is given.

II. SHALLOW-DONOR-IMPURITY PROPERTIES

Far-infrared studies of shallow-donor-impurity transitions in n-GaAs[2,3] have indicated that the simple hydrogenic model gives a fairly accurate description of the impurity energy levels. CdTe is similar to GaAs in that it is a zinc-blende material characterized by a conduction-band minimum at $k = 0$ and an isotropic electron effective mass. Thus, it is reasonable to use the simple hydrogenic model to predict the zero-field impurity-transition frequencies in n-CdTe. We are particularly interested in the $(1s \rightarrow 2p)$ transition since it is the strongest transition and also because the Zeeman splitting of this transition can be very accurately calculated by variational methods in the hydrogenic model.[4] According to the simple hydrogenic model the $(1s \rightarrow 2p)$ transition frequency in zero magnetic field is given by

$$E_{2p} - E_{1s} = \tfrac{3}{4} R \ , \tag{1}$$

where R, the effective rydberg, is given by

$$R = \mathcal{R} m^*/m_e \epsilon_0^2 \ . \tag{2}$$

Here $\mathcal{R}$ is the atomic rydberg (13.6 eV), m^* is the effective band mass of the electron, m_e is the free-electron mass, and ϵ_0 is the low-frequency dielectric constant. In applying the hydrogenic model to

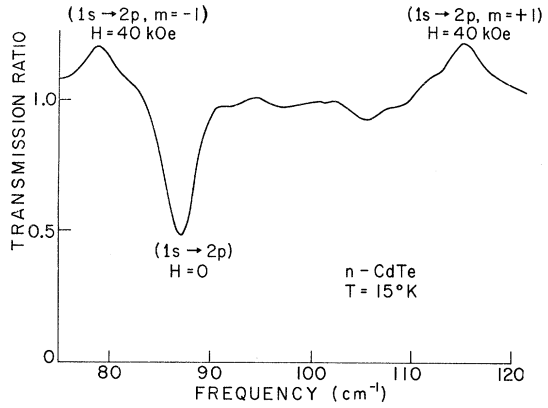

FIG. 1. Ratio of the transmission spectrum of n-CdTe at $H=0$ to the transmission spectrum at $H=40$ kOe.

CdTe we take m^*/m_e to be equal to 0.0963 ± 0.0008 (determined by millimeter cyclotron resonance)[5] and the value of the low-frequency dielectric constant to be 9.6 ± 0.2.[6] From Eqs. (1) and (2) one expects that

$$E_{2p} - E_{1s} = \tfrac{3}{4}(114 \pm 4 \text{ cm}^{-1}) = 86 \pm 3 \text{ cm}^{-1} . \quad (3)$$

In order to look for far-infrared absorption in n-CdTe the transmission of a sample 2.6 mm thick was measured with a Fourier-transform spectrometer. The sample was an undoped, zone-refined crystal with a peak mobility greater than 30 000 $\text{cm}^2\text{V}^{-1}\text{sec}^{-1}$ and a room-temperature carrier concentration of approximately 5×10^{15} cm^{-3}.

By taking the ratio of the transmitted-intensity spectrum at zero field to that obtained at sufficiently high magnetic field it is possible to discriminate against field-independent absorption and to measure separately zero-field and "high"-field absorption lines. An example of such a ratio spectrum is shown in Fig. 1, where the "high" magnetic field spectrum was taken at $H=40$ kOe. The zero-field ($1s \rightarrow 2p$) transition appears as a valley in Fig. 1, where a minimum is found to occur at 87.3 ± 0.3 cm^{-1}, in good agreement with the prediction of the hydrogenic model.

Since our transmission measurements were performed in the Faraday configuration, the presence of the magnetic field splits the ($1s \rightarrow 2p$) transition into the two observable components ($1s \rightarrow 2p$, $m = \pm 1$). These components are seen in Fig. 1 as peaks at 79.0 and 115.5 cm^{-1}.

The strength of the 87.3-cm^{-1} absorption at zero field was found to decrease as the temperature was increased—a temperature dependence which is qualitatively consistent with our identification of this absorption as an impurity transition. The absorption at 20 °K was found to be about 20% greater than that at 60 °K. Since kT at 60 °K (which is equal to 42 cm^{-1}) is only 36% of the impurity binding energy we would not expect that all of the donors would be ionized at this temperature.[7] No attempt was made to identify the chemical nature of the shallow-donor impurity or impurities.

Figure 2 shows the absorption coefficient $\alpha(\omega)$ corresponding to the ratio of the transmission spectra in Fig. 1. It is calculated from the equation

$$R(\omega) = e^{-\alpha(\omega)d} ,$$

where $R(\omega)$ is the measured ratio of the transmission spectra, and d is the thickness of the sample. We see that the full width at half-maximum of the zero-field ($1s \rightarrow 2p$) absorption coefficient is about 4.5 cm^{-1}.

The observation of the ($1s \rightarrow 2p$) transition at 87.3 ± 0.3 cm^{-1} implies that the effective rydberg is equal to 116 cm^{-1} if we neglect central-cell corrections.[8,9] Therefore, we expect that the zero-field ($1s \rightarrow 3p$) absorption should occur at $\frac{8}{9}$(116 cm^{-1}) = 103 cm^{-1}. There is in fact a small dip in Fig. 1 at about 105 cm^{-1}. However, the magnitude of this dip is only slightly greater than the noise level. Hence our identification is not conclusive.

In Fig. 3 we have plotted the experimentally determined magnetic field dependence on the ($1s \rightarrow 2p$, $m = \pm 1$) transition frequencies. Fields as high as 165 kOe, which is the limit for conventional Bitter solenoids, were employed. The size of the dots representing the experimental points is larger than

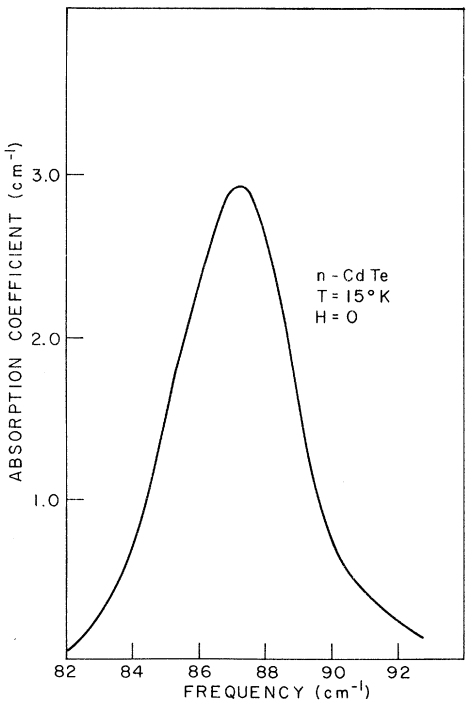

FIG. 2. Frequency dependence of the absorption coefficient for the ($1s \rightarrow 2p$) transition in n-CdTe at $H=0$.

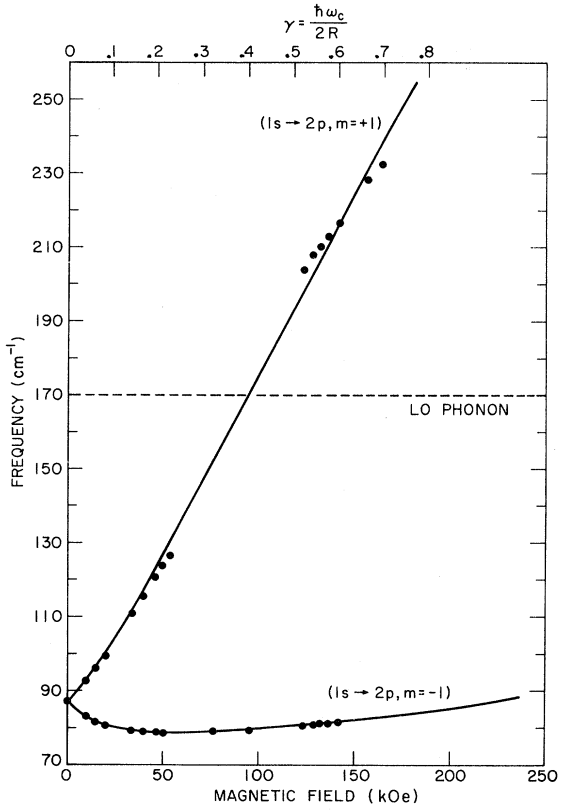

FIG. 3. Plot of the experimentally determined magnetic field dependence of the ($1s \rightarrow 2p$, $m = \pm 1$) transition frequencies in n-CdTe. The solid lines represent the predictions of Larsen's variational calculation for the shallow-donor-impurity states.

the experimental error. In general, the experimental error in the determination of the absorption frequency was ± 0.3 cm^{-1}. The magnetic field values are accurate to within 0.5%. The positions of impurity absorptions were found to be independent of temperature in the range 1.4–30 °K. It was not possible to observe the ($1s \rightarrow 2p$, $m = \pm 1$) absorptions in the 130–200-cm^{-1} region due to strong restrahlen absorption.

The solid lines in Fig. 3 represent the theoretically predicted magnetic field dependence of the ($1s \rightarrow 2p$, $m = \pm 1$) transition frequencies based upon the variational calculation of Larsen[4] for the Zeeman splitting of a hydrogenic atom. This calculation includes a correction for nonparabolicity but does not include the effect of the electron–LO-phonon interaction.[10] The theoretical curves were calculated using the value of $(0.0963 \pm 0.0008)m_e$ for the CdTe effective mass[5] and a value for the rydberg which was adjusted to bring theory and experiment into agreement at zero magnetic field ($R = 116.0$ cm^{-1}). Although it is likely that some donor-central-cell correction exists, this effect is expected to cause only very small monotonic deviations from a theoretical fit based entirely on the effective-mass approximation.[8,9] In Fig. 3 no attempt was made to correct for central-cell effects.

Although the experimentally determined magnetic field dependence of the ($1s \rightarrow 2p$, $m = -1$) transition agrees well with the theory, the agreement is distinctly poorer for the ($1s \rightarrow 2p$, $m = +1$) transition, where significant deviations occur. These deviations result from the electron–LO-phonon interaction. We will show in the next sections that a careful study of these deviations makes it possible to determine quantitatively the effect of this interaction.

III. POLARON EFFECTS: QUALITATIVE FEATURES

As we have already pointed out, electronic energy levels in polar crystals are shifted by the electron–LO-phonon interaction. These perturbations are called polaron effects; they will be particularly marked for the higher-energy member of a pair of levels whose energy separation is close to the long-wavelength, LO-phonon energy $\hbar\omega_0$. In some cases it is possible to "tune" the separation of a pair of electronic levels by means of applied magnetic field or stress and observe the magnitude of the relative level shift as the (theoretical) separation of the unshifted levels approaches $\hbar\omega_0$ from below and then exceeds this value. Experiments of this kind demonstrate a characteristic discontinuity of the level separation at $\hbar\omega_0$ which has been called the polaron-pinning effect.

The first experimental observation of pinning was made in InSb,[11] and the effect has been studied extensively in this material.[12–15] Because of the low conduction-band mass in InSb, the electronic levels are relatively easy to tune to the required separations in a magnetic field. However, InSb is so very weakly polar that polaron effects are observable only when the level separations are very close to $\hbar\omega_0$. Although serious quantitative calculations of polaron shifts in InSb have been attempted[16,17] the results cannot be considered reliable. Perhaps the most important reason is that the polaron shifts should be quite sensitive to the degree of homogeneous broadening of the lower state of the pair when the pair is separated by an energy very close to $\hbar\omega_0$. This effect has not been considered in either Ref. 16 or Ref. 17. It should be relatively important in cyclotron resonance.[18] Furthermore, in the InSb impurity-pinning experiments the impurity ground state and an infinite number of excited impurity levels are crowded into an energy interval ΔE (with $\Delta E \ll \hbar\omega_0$) just below the bottom of the $n = 0$ Landau band. In Ref. 17 only a few of these states are taken into account; it is hard to see how to include the rest, and yet also hard to see *a priori* why they should be ne-

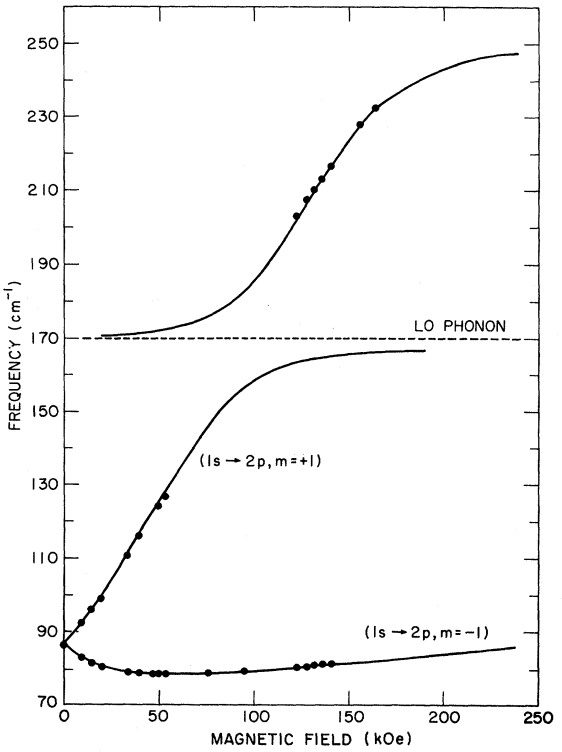

FIG. 4. Plot of the experimentally determined magnetic field dependence of the ($1s \rightarrow 2p$, $m = \pm 1$) transition frequencies in n-CdTe. The solid lines represent the predictions of the theoretical calculation for the effect of electron–LO-phonon interaction upon the shallow-donor-impurity levels. α is taken to be 0.4.

glected.

Because CdTe is much more polar than InSb and because the impurity levels do not bunch up in energy near the impurity ground state, polaron effects can be observed at level separations quite far from $\hbar\omega_0$, where neither of the objections above have any force. Thus from the point of view of the theorists CdTe is a "cleaner" material than InSb for the study of polaron effects.

The first quantitative check on the validity of the Fröhlich model of electron–LO-phonon interaction was made by Waldman *et al.* [19] who measured the cyclotron-resonance-absorption fields in n-CdTe at a number of fixed incident-photon frequencies below ω_0. Polaron shifts were observed at frequencies as small as $0.3\omega_0$. One would expect that shifts similar in magnitude to those found in cyclotron resonance could be observed in the magneto-optical spectrum of the donor.

The behavior of hydrogenic donor levels in relatively weak magnetic fields and unperturbed by polaron effects is known experimentally from magneto-optical measurements in GaAs. [2,3] This material is, like InSb, only very slightly polar so that to a good approximation the donor energy levels are unaffected by polaron shifts (except, of course, when pairs of levels become separated in energy by $\sim\hbar\omega_0$). Furthermore, quite accurate variational wave functions are available for some of the low-lying hydrogenic levels. [4]

It is not difficult to understand qualitatively the direction of the deviations of the experimental points in Fig. 3 from the transition energies expected for the case of vanishing electron–LO-phonon interaction. Second-order perturbation theory (to be discussed in Sec. IV) tells us that as a result of the electron–LO-phonon interaction a given unperturbed level l will be repelled by the one-phonon virtual state located at the energy $E_n + \hbar\omega_0$, where E_n is an unperturbed energy level of the hydrogenic atom in the magnetic field. Thus, each unperturbed level is repelled by an infinite number of levels. The strength of the repulsion is proportional to $|(E_l - E_n - \hbar\omega_0)^{-1}|$ times a squared matrix element. As E_l approaches $E_n + \hbar\omega$, the repulsion effect clearly becomes stronger and stronger. Hence, in Fig. 3 the $2p$, $m = +1$ state is seen to be pushed down in energy as it approaches $E_{1s} + \hbar\omega_0$ (dotted line) from below and pushed up as it approaches this energy from above. At higher fields the $2p$, $m = +1$ level starts to approach $E_{2p,m=-1} + \hbar\omega_0$ from below and is therefore again pushed down in energy. Results of quantitative calculations are represented by solid curves of Fig. 4, where the effect of the repulsion from $E_{2p,m=0} + \hbar\omega$ is also taken into account.

Another way to convince oneself that the electron–LO-phonon interaction is playing an important role in the data of Fig. 3 is to plot the observed energy difference $E_{2p,m=+1} - E_{2p,m=-1}$ as a function of magnetic field (see Figs. 5 and 6). What is particularly interesting about such plots is that in the absence of band nonparabolicity and electron-phonon interaction this energy difference is given by [4]

$$E_{2p,m=+1} - E_{2p,m=-1} = \hbar\omega_c \tag{4}$$

for all values of the magnetic field B, where ω_c is the parabolic-band cyclotron frequency given by

$$\omega_c = eB/m^*c \ . \tag{5}$$

Equation (4) states an exact result, not one which depends on our particular choice of variational trial functions. Moreover, the presence of central-cell corrections can hardly affect the validity of this equation because the wave functions corresponding to the $2p$, $m = \pm 1$ states, having odd parity, vanish at the donor center. Thus, measurements of the Zeeman splitting defined in Eq. (4) should provide a clean way of isolating polaron phenomena. Such measurements are shown in Figs. 5 and 6.

Although it is almost possible to pass a straight

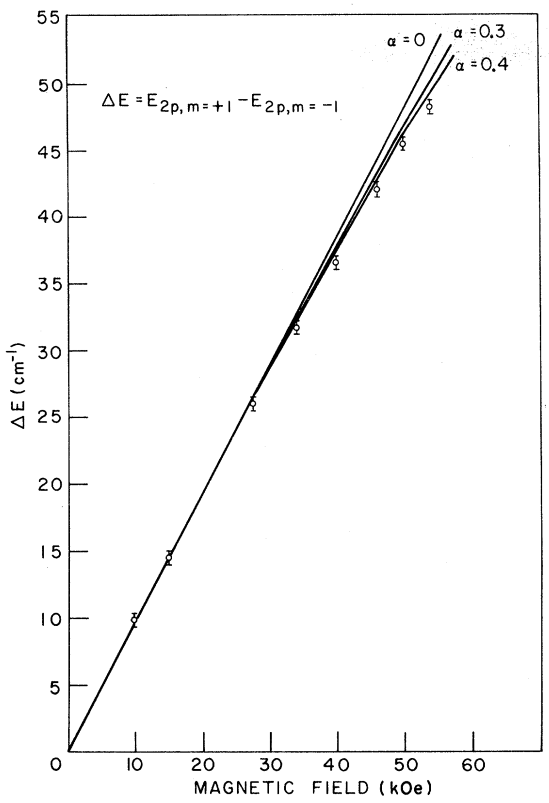

FIG. 5. Plot of the experimentally determined magnetic field dependence of $\Delta E_g = E_{2p,m=+1} - E_{2p,m=-1}$ for ($1s \rightarrow 2p$, $m=+1$) transition frequencies below the LO-phonon frequency. The solid lines represent the predictions of the theoretical calculation for the effects of electron-phonon interactions characterized by $\alpha=0$, $\alpha=0.3$, and $\alpha=0.4$.

line through the experimental points and the origin in Fig. 5, the slope of any such line would be too small for (5) to be obeyed. In Fig. 6 any straight line through the experimental points has a large, positive, zero-field intercept (in the neighborhood of 40 cm^{-1}) and a slope which is much smaller than expected on the basis of (5). Furthermore, band nonparabolicity alone cannot account for these effects as shown by the curves marked $\alpha=0$ in the figures, where nonparabolic effects are included.

Before turning to discussion of quantitative calculations of the polaron shifts we wish to point out that the experimental data displayed in Fig. 3 can be used to determine whether the electron–TO-phonon interaction plays a role in perturbing the donor levels. Previous studies in InSb have given contradictory results regarding this possibility.[14,15] If a long-wavelength, electron–TO-phonon interaction were present in any significant strength the $2p$, $m=+1$ state would be coupled to the $2p$, $m=-1$ plus one TO-phonon states. This coupling would result in strong pinning effects in the magnetic field region near 151 kOe, where the unperturbed energies of these states are nearly equal. For this range of magnetic field the ($1s \rightarrow 2p$, $m=+1$) transition energy is ~225 cm^{-1}. As can be seen in Fig. 3 the behavior of the ($1s-2p$, $m=+1$) transition shows no indication of any pinning effects in this frequency region.

IV. WEAK-COUPLING THEORY OF THE POLARON ZEEMAN EFFECT

The Frölich Hamiltonian[20] H for the coupled impurity-phonon system can be written, neglecting band nonparabolicity,

$$H = H_1 + H_2 + H_3 , \tag{6}$$

where H_1 is the Hamiltonian for the hydrogenic donor electron in a magnetic field, H_2 is the energy operator for the LO phonons, and H_3 is the Fröhlich electron-phonon-coupling interaction. Thus, we have

$$H_1 = [\vec{p} - (e/c)\vec{A}]^2/2m^* - (e^2/\epsilon_0 r) , \tag{7}$$

$$H_2 = \hbar\omega_0 \sum b_{\vec{k}}^{\dagger} b_{\vec{k}} , \tag{8}$$

$$H_3 = \left(\frac{2\pi\hbar\omega e^2}{\bar{\epsilon} V}\right)^{1/2} \sum_k \frac{1}{k} \left(e^{-i\vec{k}\cdot\vec{r}} b_{\vec{k}}^{\dagger} + e^{i\vec{k}\cdot\vec{r}} b_{\vec{k}}\right) . \tag{9}$$

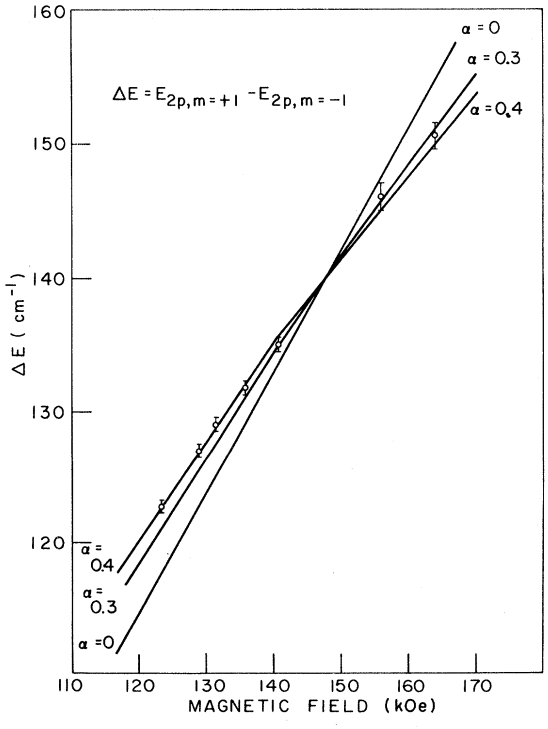

FIG. 6. Plot of the experimentally determined magnetic field dependence of $\Delta E_g = E_{2p,m=+1} - E_{2p,m=-1}$ for ($1s \rightarrow 2p$, $m=+1$) transition frequencies above the LO-phonon frequency. The solid lines represent the predictions of the theoretical calculation for the effects of electron-phonon interactions characterized by $\alpha=0$, $\alpha=0.3$, and $\alpha=0.4$.

In the above equation $\vec{A}$ is the vector potential for the applied magnetic field, $\hbar\omega_0$ is the energy of a long-wavelength LO phonon, $b_{\vec{k}}^{\dagger}$ is the creation operator for an LO phonon of wave vector $\vec{k}$, V is the crystal volume, and the effective dielectric constant $\bar{\epsilon}$ characterizing the lattice polarizability, is given in terms of the high- and low-frequency dielectric constants ϵ_∞ and ϵ_0, respectively, by

$$\frac{1}{\bar{\epsilon}}=\frac{1}{\epsilon_\infty}-\frac{1}{\epsilon_0}\ . \tag{10}$$

To simplify the notation we write Eqs. (7)–(9) in "polaron units" wherein energies are measured in units of $\hbar\omega_0$ and lengths in units of the "polaron radius" r_p defined by $r_p=(\hbar/2m^*\omega_0)^{1/2}$. Employing these units we write Eqs. (7)–(9) as

$$H_1=\hat{\pi}^2-2R_p^{1/2}/r\ , \tag{11}$$

$$H_2=\sum b_{\vec{k}}^{\dagger}b_{\vec{k}}\ , \tag{12}$$

$$H_3=\sum \nu_k\left(e^{-i\vec{k}\cdot\vec{r}}b_{\vec{k}}^{\dagger}+e^{i\vec{k}\cdot\vec{r}}b_{\vec{k}}\right)\ , \tag{13}$$

where

$$\hat{\pi}=\left(-i\frac{\partial}{\partial x}-\frac{\omega_c}{4\omega_0}y,\ -i\frac{\partial}{\partial y}+\frac{\omega_c}{4\omega_0}x,\ -i\frac{\partial}{\partial z}\right),$$

$$R_p=\frac{1}{2}\frac{m^*e^4}{\epsilon_0^2\hbar^2}\left(\frac{1}{\hbar\omega_0}\right)=\text{impurity } 1s \text{ binding energy divided by } \hbar\omega_0\ ,$$

$$\nu_k=\left(\frac{4\pi\alpha}{V/r_p^3}\right)^{1/2}\frac{1}{k}\ ,$$

and

$$\alpha=\frac{1}{2}\left(\frac{1}{\epsilon_\infty}-\frac{1}{\epsilon_0}\right)\frac{1}{\hbar\omega_0}\frac{e^2}{r_p}\ . \tag{14}$$

Our procedure is to treat H_3 as a perturbation on the eigenstates of H_1+H_2 in a modified and simplified form of second-order Wigner-Brillouin (WB) perturbation theory. We start from the WB expression for the perturbed energy of the ith level of a hydrogenic atom in a magnetic field of strength B:

$$\mathcal{E}_i(B)=E_i(m^*,B)+\frac{V}{(2\pi r_p)^3}\times\sum_n\int\frac{d^3\vec{k}\nu_k^2|\langle n|e^{-i\vec{k}\cdot\vec{r}}|i\rangle|^2}{\mathcal{E}_i(B)-E_n(B)-1}\ . \tag{15}$$

Here $E_i(m^*,B)$ represents the unperturbed ($\alpha=0$) energy of an eigenstate of H_1. The independent variable m^* is at this point redundant; it reminds us that that level E_i is calculated from H_1 in (7) using the band mass m^*.

There are a number of obstacles preventing us from evaluating (15) exactly. Not the least of these is that we do not know the energies and wave functions of all the impurity states. Nevertheless, it is possible to evaluate (15) approximately in such a way that we need only know the $1s$, $2p_{m=\pm1}$ and $2p_{m=0}$ wave functions as a function of B in order to calculate the level shifts relevant to the interpretation of our data.

To do this we iterate the identity

$$\frac{1}{E_n-\mathcal{E}_i+1}\equiv\frac{1}{1+k^2}\left(1-\frac{E_n-\mathcal{E}_i-k^2}{E_n-\mathcal{E}_i+1}\right) \tag{16}$$

to obtain[21]

$$\frac{1}{E_n-\mathcal{E}_i+1}\equiv\frac{1}{1+k^2}\left(1-\tilde{\delta}_n+\tilde{\delta}^2-\frac{\tilde{\delta}_n^3(1+k^2)}{E_n-\mathcal{E}_i+1}\right)\ , \tag{17}$$

where

$$\tilde{\delta}=(E_n-\mathcal{E}_i-k^2)/(1+k^2)\ .$$

In the present experiment $\mathcal{E}_i$ does not deviate very strongly from E_i, its unperturbed value, so that we can replace $\mathcal{E}_i$ by E_i in those terms of (17) which are not sensitive to which of these quantities are used. Thus, in (17) we approximate $1-\tilde{\delta}_n+\tilde{\delta}_n^2$ by $1-\delta_n+\delta_n^2$ where

$$\delta_n=(E_n-E_i-k^2)/(1+k^2)\ . \tag{18}$$

Using Eqs. (17) and (18), we rewrite Eq. (15) as

$$\mathcal{E}_i(B)-E_i(m^*B)=T_1+T_2+T_3+T_4\ , \tag{19}$$

where

$$T_1=-\sum_n\frac{\Omega}{(2\pi)^3}\int d^3\vec{k}\nu_k^2\frac{|\langle i|e^{-i\vec{k}\cdot\vec{r}}|n\rangle|^2}{1+k^2}d^3k\ , \tag{20}$$

$$T_2=\sum_n\frac{\Omega}{(2\pi)^3}\int d^3\vec{k}\nu_k^2\frac{|\langle i|e^{-i\vec{k}\cdot\vec{r}}|n\rangle|^2}{1+k^2}\delta_n\ , \tag{21}$$

$$T_3=-\sum_n\frac{\Omega}{(2\pi)^3}\int d^3\vec{k}\nu_k^2\frac{|\langle i|e^{-i\vec{k}\cdot\vec{r}}|n\rangle|^2}{1+k^2}\delta_n^2\ , \tag{22}$$

$$T_4=\sum_n\frac{\Omega}{(2\pi)^3}\int d^3\vec{k}\nu_k^2\frac{|\langle i|e^{-i\vec{k}\cdot\vec{r}}|n\rangle|^2}{\mathcal{E}_i(B)-E_n(m^*,B)-1}\tilde{\delta}_n^3\ , \tag{23}$$

with

$$\Omega=V/r_p^3\ .$$

In the Appendix we show how $T_1+T_2+T_3$ can be evaluated exactly. Here we merely quote the result

$$\mathcal{E}_i(B)=-\alpha+E_i(m^*,B)-\tfrac{1}{6}\alpha\langle i|\hat{\pi}^2|i\rangle+T_4\ . \tag{24}$$

Since $E_i(m^*,B)=\langle i|\ \hat{\pi}^2-2R^{1/2}/r\ |i\rangle$ we can write (24) as

$$\mathcal{E}_i(B)=-\alpha+\langle i|(1-\tfrac{1}{6}\alpha)\hat{\pi}^2-2R^{1/2}/r\ |i\rangle+T_4$$

$$\cong-\alpha+E(m^{**},B)+T_4\ ,$$

where m^{**} = polaron mass = $(1+\frac{1}{6}\alpha)m^*$.

So far, although we have made some small approximations on (15), we have not really produced any simplification, since T_4 is as difficult to evaluate exactly as the original perturbation expression. However, we expect contributions of all states $|n\rangle$ to T_4 to be small except for the states for which the energy denominator in (23) is small. The reason for this is that the matrix elements $|\langle i|e^{-i\vec{k}\cdot\vec{r}}|n\rangle|^2$ in (23) should tend to be peaked at those values of k such that $E_n - E_i \cong E_n - \mathcal{E}_i \approx k^2$. This means that $\tilde{\delta}_n^3$ should be small where the matrix element is biggest, and unless a term in the sum on n in (23) is enhanced by a small energy denominator, its contribution to T_4 can be neglected.

If the initial unperturbed state $|i\rangle$ is taken to be the $1s$ state, the term T_4 can be entirely neglected, according to this argument. Likewise in this experiment the $1s \rightarrow 2p_{m=-1}$ transition energy is always substantially smaller than $\hbar\omega_0$, and T_4 can be neglected (although in calculating the $2p_{m=-1}$ level for Fig. 4 we have, in fact, included the contribution of the $1s$ state in T_4, neglecting all other states). On the other hand, in calculating the energy of the $2p_{m=+1}$ state we have replaced the sum on $|n\rangle$ in T_4 by a sum of the three terms representing the contributions of the $1s$, $2p_{m=-1}$, and $2p_{m=0}$ states to the value of T_4.

A further approximation to T_4 which we have made is to replace $E_n(m^*, B)$ in the denominator by the renormalized energies $-\alpha + E_n(m^{**}, B)$. In this way we have sought to include some of the effects from higher-order perturbation corrections.[22]

All wave functions used in evaluating matrix elements were calculated at each field of interest using variational trial functions of the type described in Ref. 4. Nonparabolic corrections were calculated by setting $\alpha = 0$ and using the method described in Ref. 4. These corrections were then added to the results of the polaron perturbation calculation to obtain the final calculated level energies.

Theoretical curves in Figs. 4–6 were computed using the value $\alpha = 0.4$ deduced from the magnetic field dependence of the polaron mass observed in cyclotron resonance experiments in CdTe. The value of the rydberg chosen was 116.0 cm^{-1}, which was determined by fitting the zero-field $1s$-$2p$ transition energy. Thus, so far as the magnetic field dependence of the transition energies is concerned, the curves shown employ no adjustable parameters. In view of this and the nature of the approximations involved, we feel that the very close agreement between theory and experiment may be somewhat fortuitous.

We must admit that the approximations introduced here in the polaron calculations are very difficult to justify from first principles. They are, rather, motivated by our experience in handling simpler polaron problems (the perturbation theory for free polarons,[22] for polarons in a Coulomb potential alone,[23] and for polarons in a magnetic field with no Coulomb field present[24]). In this connection it is important to realize that except for our truncation of T_4, none of our approximations alter the behavior of the original perturbation expression (15) to order α as $\alpha \rightarrow 0$, at least in the magnetic field transition-energy regions of interest in this experiment.

Our expansion procedure for obtaining (19) from (15) before truncating means intuitively that we are extracting *some* contribution to the perturbed energy from each term of the sum on n in (15) while taking the exact contribution of only a few of these terms. [Using a simple coupled-mode approach,[17] that is, truncating (15) directly, we have been unable to produce a satisfactory fit to the experiment.]

Perhaps our most important approximation is the truncation of T_4. The accuracy of this approximation has been studied in detail for the weak-coupling ground-state energy in two limiting cases: (a) finite magnetic field, zero Coulomb field[25] and (b) zero magnetic field, finite Coulomb field.[26] For case (a) completely neglecting T_4 (which constitutes the weak coupling-polaron effective-mass approximation) is found very accurate when $\hbar\omega_c \lesssim \hbar\omega_0$, while the same approximation in case (b) leads to an excellent ground-state energy when $R \lesssim \hbar\omega_0$. Since no pinning can occur for the ground states, it is not necessary to save any terms in T_4 in the ground-state calculations. In view of these results we can reasonably expect that our truncation procedure will lead to quite accurate energy levels for CdTe donors in the range of magnetic fields studied here.

We obtain a better fit using $\alpha = 0.4$ than using $\alpha = 0.28$, the value which one would infer from Fröhlich's formula (14). This interesting result is consistent with the cyclotron-resonance findings of Waldman and co-workers.[19] Nevertheless, we would want to be more confident of the accuracy of our theory for the bound polaron in a magnetic field before drawing any far reaching conclusions about the validity of the Fröhlich Hamiltonian in CdTe.[27]

ACKNOWLEDGMENTS

We are indebted to Dr. H. H. Woodbury of the General Electric Research Laboratories for providing the CdTe sample used in these experiments. We also want to thank Professor Jerry Waldman for many profitable discussions and John D. Christensen for his assistance in performing the experimental measurements.

APPENDIX

We show here how to evaluate terms T_1, T_2, and T_3 exactly. By completeness, we have

$$T_1 = -(\alpha/2\pi^2)\int[d^3\vec{k}/k^2(1+k^2)] = -\alpha\,. \tag{25}$$

In order to evaluate T_2, we note that

$$\sum_n (E_n - E_i - k^2)\left|\langle i|e^{-i\vec{k}\cdot\vec{r}}|n\rangle\right|^2 = \sum_n (E_n - E_i)\langle i|e^{i\vec{k}\cdot\vec{r}}|i\rangle - k^2\,, \tag{26}$$

$$\sum_n (E_n - E_i)\langle i|e^{-i\vec{k}\cdot\vec{r}}|n\rangle\langle n|e^{i\vec{k}\cdot\vec{r}}|i\rangle = \langle i|[e^{-i\vec{k}\cdot\vec{r}}, H_1]e^{i\vec{k}\cdot\vec{r}}|i\rangle = \langle i|H_1(\hat{\pi}+\vec{k}) - H_1(\hat{\pi})|i\rangle = \langle i|k^2 - 2\vec{k}\cdot\hat{\pi}|i\rangle\,. \tag{27}$$

Now any impurity state $|i\rangle$ has a definite parity. Hence,

$$-\langle i|2\vec{k}\cdot\hat{\pi}|i\rangle = 0\,. \tag{28}$$

Using Eqs. (27) and (28) in conjunction with Eq. (26) gives

$$\sum_n (E_n - E_i - k^2)\left|\langle i|e^{-i\vec{k}\cdot\vec{r}}|n\rangle\right|^2 = \langle i|k^2|i\rangle - k^2 = k^2 - k^2 = 0\,. \tag{29}$$

Therefore, $T_2 = 0$.

We now evaluate term T_3 noting that

$$\sum_n (E_n - E_i - k^2)^2\left|\langle i|e^{-i\vec{k}\cdot\vec{r}}|n\rangle\right|^2 = \sum_n (E_n - E_i)^2\left|\langle i|e^{-i\vec{k}\cdot\vec{r}}|n\rangle\right|^2 - \sum_n 2k^2(E_n - E_i)\left|\langle i|e^{-i\vec{k}\cdot\vec{r}}|n\rangle\right|^2 + k^4\,. \tag{30}$$

The first term in Eq. (30) can be evaluated as follows:

$$\begin{aligned}\sum_n (E_n - E_i)^2\left|\langle i|e^{-i\vec{k}\cdot\vec{r}}|n\rangle\right|^2 &= \sum_n (E_n - E_i)^2\langle i|e^{-i\vec{k}\cdot\vec{r}}|n\rangle\langle n|e^{i\vec{k}\cdot\vec{r}}|i\rangle \\ &= \langle i|[[e^{-i\vec{k}\cdot\vec{r}}, H_1], H_1]e^{i\vec{k}\cdot\vec{r}}|i\rangle = -\langle i|(2\vec{k}\cdot\hat{\pi} + k^2)^2|i\rangle \\ &= \langle i|4(\vec{k}\cdot\hat{\pi})^2|i\rangle + \langle i|4k^2(\vec{k}\cdot\hat{\pi})|i\rangle + k^4\,.\end{aligned} \tag{31}$$

Using Eq. (28) in conjunction with Eq. (31) we find that

$$\sum_n (E_n - E_i)^2\left|\langle i|e^{-i\vec{k}\cdot\vec{r}}|n\rangle\right|^2 = 4\langle i|(\vec{k}\cdot\hat{\pi})^2|i\rangle + k^4\,. \tag{32}$$

Equations (27) and (28) give the result

$$-\sum_n 2k^2(E_n - E_i)\left|\langle i|e^{-i\vec{k}\cdot\vec{r}}|n\rangle\right|^2 = -2k^4\,. \tag{33}$$

Using Eqs. (32) and (33) in conjunction with Eq. (30) we then obtain

$$\sum_n (E_n - E_i - k^2)^2\left|\langle i|e^{-i\vec{k}\cdot\vec{r}}|n\rangle\right|^2 = 4\langle i|(\vec{k}\cdot\hat{\pi})^2|i\rangle\,. \tag{34}$$

Hence, we see that

$$T_3 = -(8\alpha/\pi)\int dk\,[\langle i|(\vec{k}\cdot\hat{\pi})^2|i\rangle/(1+k^2)^3]\,. \tag{35}$$

Upon performing the required integration we find that

$$T_3 = -\tfrac{1}{6}\alpha\langle i|\hat{\pi}^2|i\rangle\,. \tag{36}$$

Having evaluated T_1, T_2, and T_3, we can now write Eq. (19) as

$$\mathcal{E}_i(B) - E_i(m^*, B) = -\alpha - \tfrac{1}{6}\alpha\langle i|\hat{\pi}^2|i\rangle + T_4\,. \tag{37}$$

---

†Work supported by the U. S. Air Force Office of Scientific Research and NSF.

*Also Physics Department, Massachusetts Institute of Technology, Cambridge, Mass. 02139.

[1]D. R. Cohn, D. M. Larsen, and B. Lax, Solid State Commun. 8, 1707 (1970).

[2]G. E. Stillman, C. M. Wolfe, and J. O. Dimmock, Solid State Commun. 7, 921 (1969).

[3]R. Kaplan, M. A. Kinch, and W. C. Scott, Solid State Commun. 7, 883 (1969).

[4]D. M. Larsen, J. Phys. Chem. Solids 29, 271 (1968).

[5]A. L. Mears and R. A. Stradling, Solid State Commun. 7, 1267 (1967).

[6]D. Berlincourt, H. Jaffe, and L. R. Shiozawa, Phys. Rev. 129, 1009 (1963).

[7]G. E. Stillman, C. M. Wolfe, and J. O. Dimmock, in *Proceedings of Third Photoconductivity Conference*, 1969 (Pergamon, New York, 1971), p. 266.

[8]H. R. Fetterman, D. M. Larsen, G. E. Stillman, P. E. Tannenwald, and J. Waldman, Phys. Rev. Letters 26, 975 (1971).

[9]G. E. Stillman, D. M. Larsen, C. M. Wolfe, and R. C. Brandt, Solid State Commun. (to be published).

[10]In Fig. 3 we have used the experimentally determined low-frequency cyclotron mass in calculating the theoretical curves. If there were no electron–LO-phonon interaction in CdTe one would expect that the data points would fall on the theoretical curves. However, since we know that the dimensionless electron–LO-phonon coupling constant α does not vanish in CdTe, the low-frequency cyclotron mass is in fact a *polaron* mass so that we have really put in part of the polaron correction by calculating the donor spectrum using the polaron mass rather than the band mass. Thus the caption $\alpha = 0$ must be understood to mean the theoretical results which would be applicable if α were zero in CdTe and yet the observed cyclotron mass remained equal to the $0.0963m_e$ value of Mears. In short, these are the curves we would have deduced if we had not known that the electron–LO-phonon interaction existed.

[11]E. J. Johnson and D. M. Larsen, Phys. Rev. Letters 16, 655 (1966).

[12]D. H. Dickey, E. J. Johnson, and D. M. Larsen, Phys. Rev. Letters 18, 599 (1967).

[13]C. J. Summers, R. B. Dennis, B. J. Wherrett, P. G. Harper, and S. D. Smith, Phys. Rev. 170, 755 (1968).

[14]D. H. Dickey and D. M. Larsen, Phys. Rev. Letters 20, 65 (1968).

[15]R. Kaplan and R. F. Wallis, Phys. Rev. Letters 20, 1499 (1968).

[16]M. Nakayama, J. Phys. Soc. Japan 27, 636 (1969).

[17]R. F. Wallis, A. A. Maradudin, I. P. Ipatova, and R. Kaplan, Solid State Commun. 8, 1167 (1970).
[18]D. M. Larsen, *Proceedings of the Tenth International Conference on the Physics of Semiconductors* (U.S. AEC, Washington, D.C., 1970), p. 151.
[19]J. Waldman, D. M. Larsen, P. E. Tannenwald, C. C. Bradley, D. R. Cohn, and B. Lax, Phys. Rev. Letters 23, 1033 (1969).
[20]H. Fröhlich, Advan. Phys. 3, 325 (1954).
[21]P. M. Platzman, Phys. Rev. 125, 961 (1962).
[22]D. M. Larsen, Phys. Rev. 144, 697 (1966).
[23]D. M. Larsen, Phys. Rev. 187, 1147 (1969).
[24]D. M. Larsen, Phys. Rev. 135, A419 (1964).
[25]D. M. Larsen, in *Proceedings of NATO Advanced Study Institute on Fröhlich Polarons* (North-Holland, Amsterdam, 1971).
[26]M. H. Engineer and N. Tzoar, Phys. Rev. (to be published).
[27]A particularly stringent test for our theory would be posed by experiments extending our study of the ($1s \rightarrow 2p$, $m = +1$) transition to the vicinity of 200 kG, where strong pinning effects should occur.

PHYSICAL REVIEW B VOLUME 6, NUMBER 4 15 AUGUST 1972

Optically Induced Parametric Instabilities in Semiconducting Plasmas

J. I. Gersten and N. Tzoar*
Department of Physics, City College of the City University of New York, New York, New York 10031
(Received 28 December 1971)

The parametric generation of plasma waves from coherent electromagnetic radiation in semiconductors is considered. Three mechanisms which lead to a parametric instability are discussed. In the first mechanism the incident-radiation frequency matches the plasmon frequency. In the second case the plasma is allowed to drift, and radiation at twice the plasma frequency induces an instability. In the third instance two beams at frequencies ω_1 and $\omega_1 - 2\omega_p$ create a parametric instability. Application of the theory to InSb indicates that it should be possible to excite all three types of instabilities with currently available technology.

I. INTRODUCTION

The parametric excitation of plasma density waves in gaseous and solid-state plasmas has been of considerable interest, both theoretically[1] and experimentally.[2] These parametric excitations describe the nonlinear coupling of a radiation field to the density oscillation modes of the plasma. Many authors have considered the joint excitation of electron plasma oscillations and ion acoustic or phonon waves in multicomponent plasmas. In such cases the radiation field couples to the system regardless of the smallness of the photon wave number. As a matter of fact one can set $k \rightarrow 0$ and still obtain the parametric instability. A direct conversion of photons to plasmons has been described by Jackson.[3] There the finite wave number of the photon plays a strategic role and the instability vanishes when $k \rightarrow 0$. The parametric instability represents the absorption of a photon with frequency ω_1 and the creation of two plasmons at $\omega_p \approx \frac{1}{2}\omega_1$. Although the direct conversion of a photon into two plasmons is of interest, no experimental observations have been reported, presumably since this is a weak instability.

In this paper we consider a new nonlinear mechanism for the direct conversion of photons into plasmons. A preliminary account of this work has been presented elsewhere.[4] It is well known that at weak field strengths this process is forbidden since a single transverse photon cannot excite a single longitudinal plasmon. Only in the presence of a surface or inhomogeneity, for example, would the breaking of translational symmetry permit such a process to proceed. Our mechanism involves the interaction of two photons to produce two plasmons. This nonlinear interaction results from the nonparabolic momentum-energy relation for a single electron.[5] Since it is a nonlinear process it becomes important when the field becomes sufficiently intense, as in the case of a laser field.

We have also calculated the down-conversion of a photon into two plasmons, similar to the case discussed by Jackson.[3] However, we consider a drifting electron gas with a nonparabolic energy-momentum relation. We obtain an instability even for the long-wavelength case, i.e., $k \rightarrow 0$. The instability grows stronger with increasing drift velocity and may become the dominant process for converting a photon, having a frequency $\omega_1 \approx 2\omega_p$ into two plasmons.

We also consider the possibility of having a stimulated down-conversion process. The incident beam consists of two waves at frequencies ω_1 and $\omega_1 - 2\omega_p$, respectively. The latter wave stimulates the down-conversion of the former wave with the emission of two plasmons.